Density functional studies on a novel double-shell fullerene C 20@C 60

ARTICLE *in* JOURNAL OF MOLECULAR STRUCTURE THEOCHEM · JULY 2005

Impact Factor: 1.37 · DOI: 10.1016/j.theochem.2005.03.057

3 AUTHORS, INCLUDING:

Fengyi Liu
Shaanxi Normal University
25 PUBLICATIONS **293** CITATIONS

SEE PROFILE

ELSEVIER

Journal of Molecular Structure: THEOCHEM 725 (2005) 17–21

THEO CHEM

www.elsevier.com/locate/theochem

Density functional studies on a novel double-shell fullerene $C_{20}@C_{60}$

Fengyi Liu[a,b], Lingpeng Meng[b], Shijun Zheng[a,b,*]

[a]*Open Laboratory of Computational Quantum Chemistry, Hebei Normal University, Hongqi Street, Shijiazhuang, Hebei Province 050091, China*
[b]*Science Faculty, Beijing University of Chemical Technology, Beijing 100029, China*

Received 23 December 2004; revised 28 February 2005; accepted 8 March 2005
Available online 31 May 2005

Abstract

Geometrical and electronic structures of the smallest potential double-shell fullerenes $C_{20}@C_{60}$ were studied by using Hartree–Fock and density functional theory (DFT) B3LYP methods. Two distinctly different highly endothermic but stable isomers are located; the fusiform one with D_{5d} symmetry is 848.22 kcal mol^{-1} lower in energy than the spherical (I_h) one. Their frontier orbital, electrostatic potential as well as the electron affinity (EA) and the ionization potential (IP) were presented to give a comprehensive description of this novel endohedral system. The inter-shell interactions between C_{20} layer and C_{60} layer in $C_{20}@C_{60}$ are proved to be 'through-bond' and 'through-space' interactions for the fusiform isomer and spherical one, respectively.

Keywords: Density functional theory; Molecular electrostatic potential; Electron affinity

1. Introduction

Since the discovery [1] and macroscopic scale synthesis [2] of C_{60}, carbon clusters have been extensively researched for the purpose of producing new materials with promising physical and chemical properties. Single-wall fullerenes from C_{20} up to C_{96} have been detected by anion photoelectron spectroscopy and mass spectroscopy [3] or synthesized in macroscopic quantities [4] and numerous theoretical calculations have been performed to characterize them [5–8]. Recently, an interesting and novel variety of carbon clusters, multi-shell fullerenes including $C_{60}@C_{240}$, $C_{240}@C_{560}$ and $C_{80}@C_{240}@C_{560}$ were observed in the laser pyrolysis carbon black [9,10] and synthesized by laser vaporization method with a yield of mixed multi-shell fullerenes up to 90% [11]. If it is possible to isolate multi-shell fullerene crystals, it is interesting to compare their properties with that of other endohedrally doped fullerenes [12–15]. Unfortunately, it is extreme difficulty to produce macroscopic quantities and isolate pure samples; therefore, theoretical studies have been playing an important role in investigating the structural and electronic properties and predicting the potential characteristics of multi-shell fullerenes as well as explaining their formation mechanisms.

$C_{20}@C_{60}$, which was first suggested by L. Türker [16], should constitute one of the simplest bucky onion-like fullerenes. In fullerene family, C_{20} is the smallest possible fullerene without hexagonal rings. It contains just 12 pentagons, in a highly strained structure. The stable isomers of C_{20} clusters consist of bowl, ring, and fullerene (cage) structures [17], each of them can be experimentally produced under suitable reaction conditions [18]. Wherein, fullerene (I_h) is the most stable conformer [17]. The structure of C_{60}, which has 20 hexagonal and 12 pentagonal rings, has been well-characterized both experimentally and theoretically [1,17]. Since the radius of C_{60} is approximately 3.5 Å, the C_{20} fullerene with a radius about 2.0 Å could be placed inside the sphere. Hence, in the present study, the structural and electronic properties of simplest multi-shell $C_{20}@C_{60}$ fullerenes were studied by using Hartree–Fock and density functional theory, and we hope our results may shed some light on the understanding of such fullerene systems.

* Corresponding author. Address: Open Laboratory of Computational Quantum Chemistry, Hebei Normal University, Hongqi Street, Shijiazhuang, Hebei Province 050091, China. Tel.: +86 311 6263381; fax: +86 310 6263269.
E-mail address: sjzheng@mail.hebtu.edu.cn (S.J. Zheng).

0166-1280/$ - see front matter © 2005 Elsevier B.V. All rights reserved.
doi:10.1016/j.theochem.2005.03.057

2. Computational methods

Geometry optimizations of $C_{20}@C_{60}$ were performed at the Hartree–Fock and DFT/B3LYP level of theory with the less sophisticated STO-3G* and 3-21G* basis sets due to the large amount of atoms. Harmonic vibrational frequencies were calculated at Hartree–Fock level to ensure true minima were located. The total energies, orbital energies and molecular electrostatic potential (MEP) were obtained from B3LYP/3-21G* calculation with SCF convergence criteria 1×10^{-8}. To get the electron affinity (EA) and the ionization potential (IP) of different isomers of $C_{20}@C_{60}$, total energies for $C_{20}@C_{60}^{+}$ and $C_{20}@C_{60}^{-}$ were also calculated at the same level. All calculations were carried out with the GAUSSIAN 98 program package [19].

3. Results and discussions

Three models, HF/STO-3G*, HF/3-21G* and B3LYP/3-21G*, were employed in geometry optimizations to obtain results at different theory levels as well as to minimize the computational cost. The single-wall fullerenes C_{20} and C_{60} were firstly optimized, and then the $C_{20}@C_{60}$ was constructed by putting C_{20} in the position of the spherical center of C_{60} along different directions. In fact, due to the inter-shell distances in $C_{20}@C_{60}$ are quite short, the carbon atoms in C_{20} layer are strongly confined by the outer-shell, as results, only two highly symmetric isomers, Isomer I (D_{5d}) and II (I_h), were located in geometry optimization at Hartree–Fock and B3LYP level. Their optimized geometries are summarized in Fig. 1 and Table 1.

From the viewpoint of double-shell fullerenes, both isomers I and II of $C_{20}@C_{60}$ show shorter inter-shell distances than the observed average inter-layer separation 3.4 Å in $C_{60}@C_{240}$ [10]. The B3LYP/3-21G* calculation gave average radii 1.988 Å for C_{20} shell and 3.814 Å for C_{60} shell in isomer I, the corresponding values in isomer II are 1.917 Å for C_{20} and 3.863 Å for C_{60} layer, while the spherical radius for free C_{20} is 2.046 Å and free C_{60} is 3.555 Å. Obviously, in both conformers of $C_{20}@C_{60}$, the inner-shells are compressed while the outer-shells are expanded due to the inter-shell repulsion caused by these over-crowded structures. It is also interesting to see from Fig. 1 that Isomer I and II have distinctly different structures: Isomer I shows an 'elongate' fusiform geometry along the *z*-axis (see Fig. 1) while Isomer II keeps the spherical structure. This structural difference between them should be illuminated by analyzing the inter-shell interactions between C_{20} and C_{60} layer in both conformers. In isomer I with D_{5d} symmetry, each atom (e.g. C(1) atom, etc.) in the top pentagon of C_{20} directs towards a corresponding carbon (e.g. C(26), etc.) in C_{60} layer, the distance between them is only 1.535 Å at B3LYP/3-21G* level and it is evidently to see the existence of inter-shell C–C bond. The formations of chemical bonds change the hybrid states of C(1) and other equivalent atoms in C_{20} layer as well as corresponding atoms (e.g. C(26)) in C_{60} layer from sp^2 to sp^3, which further weaken the tensility and conjugation in the hexagons of C_{60} layer. As results, the C(26) and other equivalent atoms are sunken-in and the topmost pentagon formed by C(21)–C(25) is pushed away from its original position in free C_{60}; the isomer I itself shows an elongated fusiform symmetry. In the symmetry-holding isomer II, each pentagon in C_{60} layer is central projected to a pentagon of inner-shell in adverse orientation

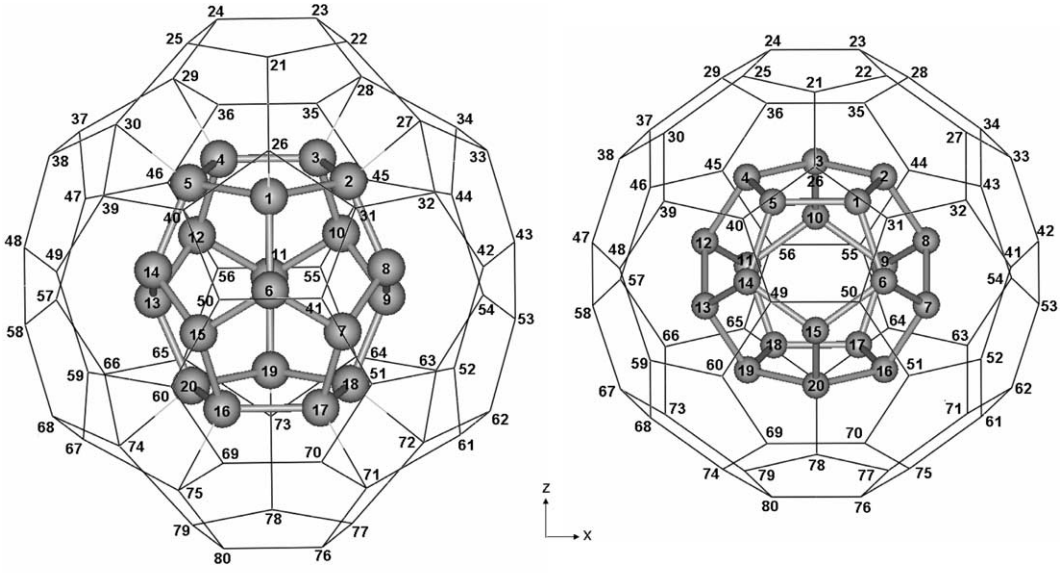

(a) Isomer I (D_{5d}) (b) Isomer II (I_h)

Fig. 1. Optimized geometries of $C_{20}@C_{60}$ isomers. The inner C_{20} shell is plotted in ball and stick and outer C_{60} shell in wire-frame.

Table 1
Optimized bond lengths and inter-shell distances (Å) of $C_{20}@C_{60}$ at Hartree–Fock and B3LYP level

Isomer	Parameter[a]	HF/ STO-3G*	HF/ 3-21G*	B3LYP/ 3-21G*
I (D_{5d})	C(1)–C(2)	1.474	1.464	1.479
	C(1)–C(6)	1.441	1.416	1.429
	C(6)–C(7)	1.421	1.345	1.362
	C(1)–C(26)	1.525	1.520	1.535
	C(21)–C(22) (h–p)[b]	1.455	1.459	1.482
	C(21)–C(26) (h–h)	1.618	1.634	1.626
	C(26)–C(31) (h–p)	1.612	1.613	1.623
	C(31)–C(32) (h–h)	1.466	1.477	1.481
	C(31)–C(41) (h–p)	1.464	1.443	1.474
	C(41)–C(50) (h–p)	1.532	1.530	1.540
	p(inner)–p(outer)[c]	2.185	2.171	2.172
	C(inner)–C=C(outer)	1.659	1.807	1.813
II (I_h)	C(1)–C(2)	1.417	1.353	1.368
	C(21)–C(22) (h–p)	1.493	1.488	1.510
	C(21)–C(26) (h–h)	1.637	1.646	1.645
	p(inner)–p(outer)	2.033	2.107	2.119
	C(inner)–h(outer)	1.508	1.598	1.609

[a] Other geometric parameters are omitted according to molecular symmetry.
[b] Position of chemical bond: h–p denotes the common border between a hexagon and pentagon and p–p means the bond belongs to two hexagon.
[c] Inter-shell distance: p(inner)–p(outer) denotes the distance between pentagons of C_{20} layer and the aspectant one of C_{60} layer; C(inner)–C=C(outer), the distance between the carbon atom of C_{20} shell and the center of C=C bond in outer C_{60} shell; C(inner)–p(outer), the distance between the inner-shell carbon and center of aspectant outer-shell hexagon.

(see Fig. 1), the repulsion between them enlarges the radius of outer-shell and compress the inner C_{20} shell. The B3LYP/3-21G* results show a inter-shell spacing about 1.95 Å, which is much larger than the radius difference of 1.51 Å between free C_{60} and C_{20} fullerenes calculated at the same level.

The total/relative energies and the atomization energies as well as the frontier orbital energies of $C_{20}@C_{60}$ are shown in Table 2. The relative energies from DFT/B3LYP calculation show Isomer I with D_{5d} symmetry locates 848.22 kcal mol^{-1}, which is lower in energy than the spherical isomer II (I_h). In fact, both isomer I and II are highly endothermic, their atomization energies per carbon, −182.07 and −171.46 kcal mol^{-1}, respectively, are evidently lower than the average value −200.23 kcal mol^{-1} of C_{60}; meanwhile, the former is slightly larger than −182.02 kcal mol^{-1} of C_{20} but the latter is less stable than C_{20}. Hence, their relative stabilities should be in the order of $C_{60} > C_{20}@C_{60}$ (D_{5d}) $> C_{20} > C_{20}@C_{60}$ (I_h). Moreover, the HOMO–LUMO gap is traditionally associated with chemical stability against electronic excitation, with larger gap corresponding to greater stability. The HOMO–LUMO gaps of Kohn–Sham orbital calculated at B3LYP/3-21G*// B3LYP/3-21G* level for isomer I and II are 1.139 and 0.885 eV, show evident reductions compared with the gap value 1.666 eV of C_{60} [20], also suggestive of the reduced stabilities from C_{60}, $C_{20}@C_{60}$ (D_{5d}) to $C_{20}@C_{60}$ (I_h).

Fig. 2 shows the three-dimensional contour diagrams of HOMO and LUMO in isomer I and II. It is seen that both the double degenerated HOMO (e_{1u}) and the LUMO (a_{1g}) orbital of isomer I have approximate equivalent contributions from inner-shell and outer-shell; while in isomer II, the main characters of HOMO (t_{1g}) orbital are from outer C_{60} layer and the dominant coefficients of LUMO (h_g) are from inner C_{20} layer. It reflects the inter-shell interactions in these conformers are different. These interactions will be discussed below on the bases of atomic charge distribution and molecular electrostatic potential.

The ionization potential (IP) and electron affinities (EA), which are directly relative to the possibilities of donating electron or accepting one electron, respectively, are also seen in Table 2. Here we give the B3LYP/3-21G*// B3LYP/3-21G* vertical values of IP and EA, the former corresponds

Table 2
Some energies of $C_{20}@C_{60}$ at B3LYP/3-21G* level based on Hartree–Fock and B3LYP optimized geometries

Isomer	Energy	B3LYP//HF[a]	B3LYP//HF[b]	B3LYP//B3LYP
I (D_{5d})	Total (Hartree)	−3028.9807460	−3029.0228152	−3029.0460924
	ΔE (kcal mol^{-1})	0.00	0.00	0.00
	Atomization (kcal mol^{-1})	−14524.51	−14550.91	−14565.51
	HOMO (eV)	5.359	5.495	5.459
	LUMO (eV)	4.237	4.248	4.319
	$\Delta E_{HOMO-LUMO}$ (eV)	1.112	1.247	1.139
	IP (eV)			6.688
	EA (eV)			3.234
II (I_h)	Total (Hartree)	−3027.5256091	−3027.6680044	−3027.6943619
	ΔE (kcal mol^{-1})	913.11	850.16	848.22
	Atomization (kcal mol^{-1})	−13611.40	−13700.75	−13717.29
	HOMO (eV)	5.920	6.154	5.882
	LUMO (eV)	4.941	5.218	4.997
	$\Delta E_{HOMO-LUMO}$ (eV)	0.979	0.936	0.885
	IP (eV)			7.356
	EA (eV)			3.931

[a] B3LYP/3-21G* energies based on HF/STO-3G*.
[b] HF/STO-3G* optimized geometries.

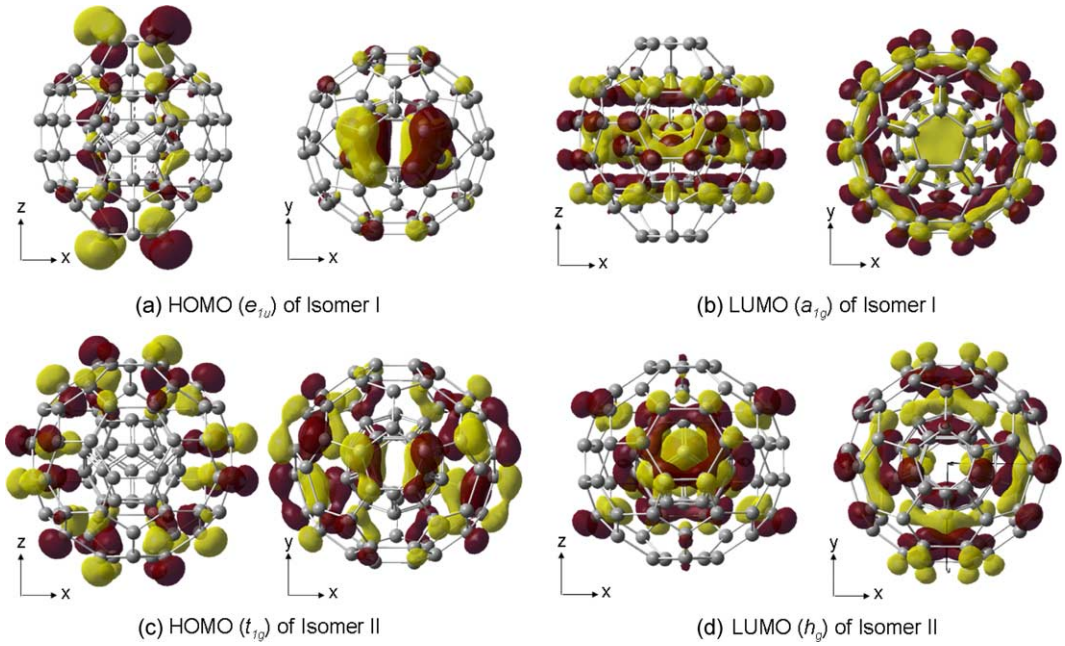

Fig. 2. Diagrams of HOMO and LUMO orbtials for C20@C60 isomers with contour value = 0.025.

to the energy difference between the cationic state in the geometry of neutral state and the optimized neutral state, whereas the latter refers to the energy difference between the optimized neutral state and anionic state in the geometry of neutral state. The VIP values are 6.688 and 7.356 eV for isomer I and II, respectively, slightly lower than 7.859 eV for C_{60} calculated at the same level. While the VEA values of these two isomers are 3.234 and 3.931 eV, respectively, evidently larger than 1.866 eV of C_{60}. These results demonstrate the stability of double-shell $C_{20}@C_{60}$ and also show it has similar possibility of both accepting and donating electrons with the single-shell C_{60} fullerene.

Table 3 lists the Mulliken atomic charges of $C_{20}@C_{60}$ calculated at different levels. The atomic changes of carbon atoms in free I_h symmetrical C_{60} and C_{20} fullerenes are all zero; however, the $C_{20}@C_{60}$ shows interesting atomic charge populations due to the structural distortions. The atoms of inner C_{20} layers in both isomers show positive charges, but those of outer-shells are quite different. In isomer I, the atoms of C_{60} layer could be divided into four kinds in which the atoms belongs to the topmost pentagon show negative charges −0.134 (e.g. C(21), etc. B3LYP/3-21G* value). It may imply the existence of 'through-bond' interactions in which the inner-C_{20} is electron donor and the two topmost/downmost pentagons in C_{60} layer are electron acceptor, their neighboring atoms, i.e. C(26) and other equivalent atoms, connecting both to the outer-layer

Table 3
Mulliken atomic charges of $C_{20}@C_{60}$ at Hartree–Fock and B3LYP level

Isomer	Atom[a]	HF/STO-3G*	HF/3-21G*	B3LYP/3-21G*
I (D_{5d})	C(1)	0.071	0.023	0.028
	C(6)	−0.047	0.020	0.023
	C(21)	−0.008	−0.015	−0.013
	C(26)	−0.152	−0.136	−0.134
	C(31)	0.079	0.076	0.072
	C(41)	−0.011	−0.022	−0.023
II (I_h)	C(1)	0.065	0.078	0.083
	C(21)	−0.022	−0.026	−0.028

[a] Atomic charges of other atoms are omitted according to molecular symmetry.

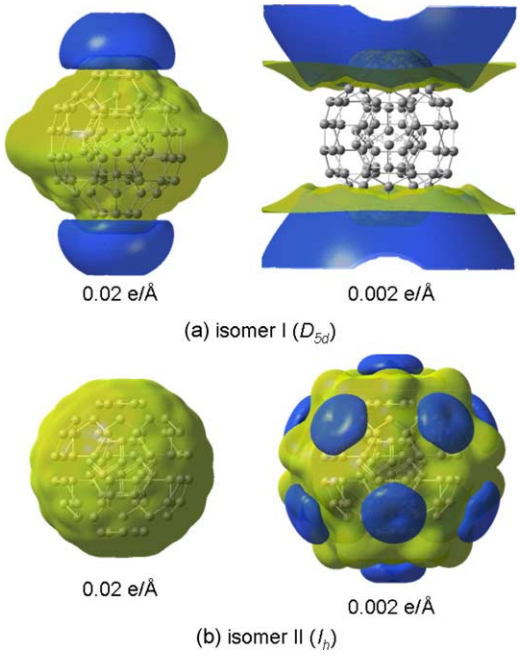

Fig. 3. Three-dimensional molecular electrostatic potential of $C_{20}@C_{60}$ isomers. The positive value is in yellow and negative value in blue. (For interpretation of the reference to colour in this legend, the reader is referred to the web version of this article.)

and to the inner layer, act as bridged-atoms in the inter-shell interaction. In isomer II, the atomic charges of C_{60} layer are −0.028 (B3LYP/3-21G* results), denotes another type of 'through-space' interactions between the pentagons in C_{20} layer (as electron donors) and C_{60} layer (as electron acceptors). That is, two different interactions could be found in different isomers of $C_{20}@C_{60}$ system.

The inter-shell interactions in $C_{20}@C_{60}$ can also be revealed by analyzing their molecular electrostatic potential (MEP). The MEP has been employed as an informative tool of chemistry to describe physical properties, molecular reactivities, and intermolecular interactions [21,22]. In particular, noncovalent molecular interactions seem likely to depend upon the patterns of the electrostatic potentials over the molecules' entire surfaces as well as the local maxima and minima. Here we introduce the MEP to describe the inter-shell interaction in $C_{20}@C_{60}$ fullerenes. The three-dimensional MEP surfaces of both conformers are plotted in Fig. 3. Both of them show quite different patterns compared with the spherical potential of C_{20} and C_{60} [16]. In isomer I, the negative potential concentrates over the surface of the upmost/downmost pentagons in C_{60} layer, while in isomer II, small negative potential regions over the pentagons of outer-shell can be seen when contour value decrease to 0.002 e/Å. In general, the negative electrostatic potentials are usually associated with the lone pairs of the more electronegative atoms and unsaturated aromatic and strained carbon–carbon bonds. It is evident that the negative MEP regions in isomer I and II are caused by the inner-pentagons π conjugations. The through-bond interactions in isomer I as well as the through-space interactions in II increase the negative charges in the certain pentagons to form anion-like 4m type π-systems, which are aromatic and stable.

4. Conclusions

In the present study, the smallest potential double-shell fullerenes $C_{20}@C_{60}$ were investigated and two distinctly different highly endothermic but stable isomers are located; the fusiform one with D_{5d} symmetry is 848.22 kcal mol^{-1} lower in energy than the spherical (I_h) one. Their frontier orbital, electron affinity (EA) and ionization potential (IP) as well as molecular electrostatic potential were presented. All results show the stability of $C_{20}@C_{60}$ and the existence of strong inter-shell interactions between C_{20} and C_{60} layers. These inter-shell interactions, which are proved to be 'through-bond' and 'through-space' interactions for the fusiform and spherical isomer, respectively, will be addressed in future studies.

Acknowledgements

This project was supported by the Nature Science Foundation of Hebei Province (Contract No. B2004000147).

References

[1] H.W. Kroto, J.R. Heath, S.C. O'Brien, R.F. Curl, R.E. Smalley, Nature 318 (1985) 162.
[2] W. Krätschmer, L.D. Lamb, K. Fostiropoulos, D.R. Huffman, Nature 347 (1990) 354.
[3] H. Kietzmann, R. Rochow, G. Ganteför, W. Eberhardt, K. Vietze, G. Seifert, P.W. Fowler, Phys. Rev. Lett. 81 (1998) 5378 and references therein.
[4] G.E. Scuseria, Science 271 (1996) 942 and references therein.
[5] J.M.L. Martin, Chem. Phys. Lett. 255 (1996) 1.
[6] F. Jensen, H. Koch, J. Chem. Phys. 108 (1998) 3213.
[7] P.R.C. Kent, M.D. Towler, R.J. Needs, G. Rajagopal, Phys. Rev. B 62 (2000) 15394.
[8] P.R. Taylor, E. Bylaska, J.H. Weare, R. Kawai, Chem. Phys. Lett. 235 (1995) 558.
[9] V.Z. Mordkovich, A.G. Umnov, T. Inoshita, M. Endo, Carbon 37 (1999) 1855.
[10] V.Z. Mordkovich, Chem. Mater. 12 (2000) 2813.
[11] V.Z. Mordkovich, Y. Takeuchi, Chem. Phys. Lett. 355 (2002) 133.
[12] J.R. Heath, S.C. O'Brien, Q. Zhang, Y. Liu, R.F. Curl, H.W. Kroto, F.K. Tittel, R.E. Snalley, J. Am. Chem. Soc. 107 (1985) 7779.
[13] R. Tegelmann, N. Krawez, S.H. Lin, I.V. Hertel, E.E. Campbell, Nature (London) 382 (1996) 407.
[14] L.S. Wang, O. Cheshnovsky, R.E. Smalley, J.P. Carpenter, S.J. Hwo, J. Chem. Phys. 96 (1992) 4028.
[15] B. Palpant, Y. Negishi, M. Sanekata, K. Miyajima, S. Nagao, K. Judai, D.M. Rayner, B. Simard, P.A. Hackett, A. Nakajima, K. Kaya, J. Chem. Phys. 114 (2001) 8459.
[16] L. Türker, J. Mol. Struct. (Theochem) 545 (2001) 207.
[17] J. Cioslowski, Electronic Structure Calculations on Fullerenes and Their Derivatives, Oxford University Press, New York, 1995.
[18] H. Prinzbach, A. Weiler, P. Landenberger, E. Wahl, J. Worth, L. Scott, M. Gelmont, D. Olevano, I. BV, Nature 407 (2000) 60.
[19] M.J. Frisch. GAUSSIAN 98, Gaussian, Inc., Pittsburgh, PA, 1998.
[20] X.Y. Ren, Z.Y. Liu, M.Q. Zhu, K.L. Zheng, J. Mol. Struct. (Theochem) 710 (2004) 175.
[21] P. Politzer, J.S. Murray, in: J.S. Murray, K.D. Sen (Eds.), Molecular Electrostatic Potentials: Concepts and Applications, Elsevier, Amsterdam, 1996.
[22] F.Y. Liu, B.L. Liu, Z.X. Meng, S.J. Zheng, J. Mol. Struct. (Theochem) 712 (2004) 207.